ResearchGate

See discussions, stats, and author profiles for this publication at: https://www.researchgate.net/publication/6210266

Vibrational Energy Exchanges in Nitrogen: Application of New Rate Constants for Kinetic Modeling

ARTICLE *in* THE JOURNAL OF PHYSICAL CHEMISTRY A · SEPTEMBER 2007

Impact Factor: 2.69 · DOI: 10.1021/jp071657a · Source: PubMed

CITATIONS
12

READS
18

4 AUTHORS, INCLUDING:

A. K. Kurnosov
Troitsk Institute for Innovation and Fusion R…
89 PUBLICATIONS **395** CITATIONS
SEE PROFILE

Anatoly P Napartovich
Troitsk Institute for Innovation and Fusion R…
610 PUBLICATIONS **3,672** CITATIONS
SEE PROFILE

S. L. Shnyrev
National Research Nuclear University MEPHI
59 PUBLICATIONS **148** CITATIONS
SEE PROFILE

Available from: Anatoly P Napartovich
Retrieved on: 25 January 2016

BATCH: jp7c14 USER: eap29 DIV: @xyv04/data1/CLS_pj/GRP_jx/JOB_i30/DIV_jp071657a DATE: July 9, 2007

Vibrational Energy Exchanges in Nitrogen: Application of New Rate Constants for Kinetic Modeling

A. Kurnosov,[†] A. Napartovich,*[,†] S. Shnyrev,[†] and M. Cacciatore*[,‡]

State Research Center, Troitsk Institute for Innovation and Fusion Research, 142190, Troitsk Moscow Region, Russia, and CNR-Institute of Inorganic Methologies and Plasmas, Bari, Department of Chemistry, University of Bari, via E. Orabona 4, 70126 Bari, Italy

Received: February 28, 2007; In Final Form: May 4, 2007

The state-to-state collisional data on vibration−vibration and vibration−translation/rotation energy exchanged in $N_2(v)-N_2(v')$ collisions recently obtained from accurate ab initio semiclassical calculations have been used to analyze the data measured in nitrogen under two different plasma conditions. In particular, the vibrational distribution function and the time-evolution of the gas temperature measured under post-discharge and glow discharge conditions, respectively, have been calculated and compared with the experimental observations. The theoretical analysis and the related results, generally in very good agreement with the experimental data, provide insight into the various energy-exchange mechanisms that lie behind the macroscopic behaviors of the nitrogen plasmas. In particular, the role played by the vibrationally excited nitrogen molecules in the gas kinetics is pointed out, as well as the importance of nitrogen atom production in the long time scales of the glow discharge.

1. Introduction

Knowledge of the vibration−vibration (V−V) and vibration−translation/rotation (V−T/R) energy exchange rates in collisions involving diatomic species such as N_2, O_2, and CO is of crucial importance for a correct description of the energy balance in the earth's atmosphere and many other technological systems, including CO/CO_2 gas lasers, plasma-chemistry reactors, and reactive hypersonic air fluxes. As a consequence, for a reliable description of the vibrational kinetics in the above-mentioned gaseous systems, there is a search for highly accurate collisional data for V−V and V−T/R energy exchanges involving vibrationally excited molecular species.[1,2]

Despite a long history, experimental determination of the relevant vibrational rate coefficients in $N_2(v)-N_2(v')$ collisions remains rather scarce. At elevated gas temperatures ($T > 500$ K), the data on the V−T relaxation rate for different measurements converge rather well,[3] whereas, at lower temperatures, the scatter of the data obtained from different sources is large.[4−7] This is partially explained by the difficulty of measuring the populations of vibrationally excited N_2 molecules in which the IR transitions are strictly forbidden.

Recently, the authors carried out a new semiclassical study on the vibrational energy exchange dynamics in $N_2(v)-N_2(v')$ collisions, and a new set of accurate state-to-state rate constants for V−V and V−T/R exchanges was calculated over a large temperature range and for a wide range of vibrational quantum numbers (v,v').[8] Compared to the V−T rate constants obtained by Billing and by Billing and Fisher in their classic works,[9,10] the newly calculated rate constants have some important behaviors and are in better agreement with the experimental data, particularly in the thermal energy regime around 500 K.

As far as the V−V energy exchange is concerned, the experimental determinations of the rate constant for the resonant transition $(0,1) \rightarrow (1,0)$ at $T = 300$ K led to a rather wide range of values: from 0.9×10^{-14} cm^3 s^{-1} [11] and 2.5×10^{-14} cm^3 s^{-1} [12,13] to 10.9×10^{-14} cm^3 s^{-1}.[14] The results of the semiclassical calculations were 1.94×10^{-14} cm^3 s^{-1} [8] and 0.9×10^{-14} cm^3 s^{-1} [9].

Indeed, the experimental works performed in refs 12−14 do not provide a direct measure of the rate coefficient, but give data (vibrational population distribution, relaxation times, etc.) from which the rate coefficients of the vibrational exchanges involved in the kinetics can be inferred by a kinetic modeling of the experiments. Generally, the applied procedures are reduced to the direct simulation of the experimental conditions, assuming as fitting parameters the rate coefficients for the relevant V−V and V−T processes as a function of the gas temperature and vibrational quantum numbers. It is a matter of fact that such procedures cannot provide an unambiguous interpretation of the experimental results. In particular, problems with the nonuniformity of excited gas and lack of gas temperature control are the main limitations in the accuracy of mathematical treatment of measured data.

Accurate measurements of the rate constants $K(1,0|v,v+1)$, $v = 0-6$ and $T = 300$ K, were recently reported in ref 11, where the stimulated Raman scattering pump and probe technique was developed to probe the vibrational population decay of selected vibrational levels (up to $v = 6$) of N_2. Comparison between the newly calculated semiclassical rate constants[8] $K(1,0|v,v+1)$, $v = 0,6$, and the V−V rate constants given by Ahn et al.[11] was made in our previous work (see Figure 7b of ref 8). These comparison shows that the difference between them is within a factor of $1.3 \div 2$.

It is the objective of the present investigation to make use of the large mass of ab initio data emerging from our previous works on the $N_2(v)-N_2(v')$ system to analyze the data measured in nitrogen under two different plasma conditions, that is,

(i) the vibrational distribution function (VDF) measured in post-discharge conditions[12,13] and

* Corresponding author. E-mail: mario.cacciatore@ba.imip.cnr.it (M.C.); apn@triniti.ru (A.N.).
[†] Troitsk Institute for Innovation and Fusion Research.
[‡] CNR-Institute of Inorganic Methodologies and Plasmas, Bari.

10.1021/jp071657a CCC: $37.00 © xxxx American Chemical Society
Published on Web 00/00/0000 PAGE EST: 8.2

BATCH: jp7c14 USER: eap29 DIV: @xyv04/data1/CLS_pj/GRP_jx/JOB_i30/DIV_jp071657a DATE: July 9, 2007

(ii) the time-evolution of the gas temperature observed in glow discharge in nitrogen.[15]

The experimental measurements[12,13,15] were numerically simulated taking the V−V and V−T rate coefficients without any fit parameters. While most of the rate coefficients were taken from ref 8, a new round of ab initio calculations were performed, and the set of the V−V and V−T rate constants enlarged to include the relaxation of the vibrational levels (v,v') not considered in ref 8. The new semiclassical rates were calculated assuming the same interaction potential and same molecular parameters as those in ref 8.

Since the dynamical behavior of the VDF is sensitive to the rate constants of the collisional processes involving vibrationally excited N_2 molecules, the experimental data measured in the two above-mentioned systems are very informative.

Therefore, the present work has two main aims: to assess the ability of the updated rate constants in modeling both the VDF and the time evolution of the gas temperature measured in N_2 plasmas, and to gain insight into the complex vibrational energy exchange mechanism that lies behind the macroscopic behaviors of N_2 in post-discharge and glow discharge conditions. The results of the vibrational kinetics modeling can also be considered as indirect evidence of the reliability of the rate constants calculated for vibrational exchanges involving the medium and high-lying vibrational levels of N_2.

2. Theoretical Modeling

2a. V−T/R and V−V Semiclassical Rate Constants. Recently, a critical revision has been made to the collisional data concerning the vibrational energy exchanges in diatom−diatom collisions, specifically for the systems involving O_2,[16] N_2,[8] CO,[17] and CO/ N_2.[18]

In particular, the N_2-N_2 system was re-examined by us[8] using an accurate semiclassical coupled-state approach to describe the collision dynamics together with an improved interaction potential $V_{int}(R, r)$ between the two interacting nitrogen molecules, with R and r being the relative distance of the two molecules and the intramolecular N−N distance, respectively. According to this method, the molecular rotations and the relative translational motion of the two N_2 molecules are treated within the classical approximation, whereas the molecular vibrations are quantized. The full collision dynamics is therefore obtained by solving the Hamilton classical equations of motion in an effective Hamiltonian of the mean field type given as the expectation value of the interaction potential V_{int} over the vibrational wave function. The Hamilton equations of motion are solved self-consistently with the time-dependent Schrodinger equations for the quantum part of the complete molecular system (see ref 2 for details).

As usual, the interaction potential was expressed as the sum of two terms: the short-range potential recently proposed in ref 19 and the attractive long-range potential obtained as a multipole expansion plus the dispersion terms. Although the accurate determination of the interaction potential for this system requires further investigations,[8] some critical aspects concerning the additivity of the different potential terms determined independently were considered, and the best performing potential in a large interaction domain was identified (at least, as far as the accuracy of the calculated vibration rate constants is concerned).

The semiclassical state-to-state rate constants were calculated by averaging the collisional cross-section over a Boltzmann distribution of the initial rotational and translational energies of the two colliding molecules:

$$K_{n_1n_2\to n_1'n_2'}(T) = \sqrt{\frac{8kT}{\mu\pi}}\left(\frac{T_0}{T}\right)^3 \int_{\epsilon_{min}}^{\infty} \sigma_{n_1n_2\to n_1'n_2'}(U)\exp\left(-\frac{\bar{U}}{kT}\right)d\left(\frac{\bar{U}}{kT}\right) \quad (2.1)$$

where U is the total classical energy defined as the sum of the rotational and translational kinetic energies of the two colliding molecules, $\bar{U}$ is the symmetrized effective energy ($\bar{U} = (1/2)\{U - (1/2)\Delta E + [U(U-\Delta E)]^{1/2}\}$), and $\Delta E = E_{n_1'} + E_{n_2'} - E_{n_1} - E_{n_2}$.

The semiclassical cross-sections $\sigma_{n_1n_2\to n_1'n_2'}$ are found by averaging over the overall mean trajectories, N_t, at a fixed value of U:

$$\sigma_{n_1n_2\to n_1'n_2'}(U) = \frac{\pi\hbar^6}{8\mu I_1 I_2 (kT_0)^3}\int_0^{l_{max}} dl \int_0^{j_{1max}} dj_1 \int_0^{j_{2max}} dj_2 \; (2j_1+1)(2j_2+1)(2l+1)\frac{1}{N_t}\sum |a_{n_1n_2\to n_1'n_2'}|^2 \quad (2.2)$$

Here, $a_{n_1n_2\to n_1'n_2'}$ are the computed single-run quantum transition amplitudes. Each trajectory is picked up randomly in the classical phase space defined by the classical action-angle variables.[2,18]

In the above equation, l is the orbital angular momentum, and j_i and I_i are the rotational angular momentum and the moment of inertia of molecule i, respectively. T_0 is an arbitrary reference temperature.

Compared to the classical data calculated by Billing, the newly calculated rate constants for the V−T/R and V−V exchanges are in a much better agreement with the available experimental data. In particular, the new rate constants exhibit different behaviors in two significant points: first, the new rates behave differently as a function of temperature, and, second, the rate constant dependence on the vibrational quantum number is also different. This second aspect is of crucial importance in the vibrational kinetic modeling of reactive or nonreactive gas systems far from thermal equilibrium conditions.

In this work, the calculations performed in ref 8 were extended so as to explore the vibrational relaxation dynamics for different vibrational transitions in N_2 and for N_2 in the higher vibrational states. Figure 1 shows the V−T rate coefficients at $T = 500$ K for the transitions $N_2(v) + N_2(v'=0) \rightarrow N_2(v-1) + N_2(v'=0)$ calculated at different vibrational quantum numbers v, with v in the range $v = 1-40$.

The ab initio rates can be well described by the simplest analytical formula exploited in the Schwartz−Slawsky−Herzfeld (SSH) theory:[1]

$$K_{v,v-1}(v) = P_{1,0}\cdot\frac{v+1}{1-(v+1)\cdot x_e}\cdot\exp(v\cdot\delta_{VT}) \quad (2.3)$$

with

$$\delta_{VT} = \frac{1.87\Delta E L^{2/3}\mu^{1/3}}{E_{1,0}^{1/3}T^{1/3}} \quad (2.4)$$

Here, x_e is the anharmonicity factor, ΔE is the energy anharmonicity (in K), $E_{1,0}$ is the exothermic energy of the vibrational transition (1→0) (in K), μ is the reduced collision mass (in a.u.), and L (in Å) is the characteristic parameter of the exponential short-range repulsive potential. The L value providing the best fit of the analytical approximation to our numerical results is equal to $L = 0.23$ Å (compared to $L = 0.203$ Å recommended in ref 20 and $L = 0.25$ Å[21]). Other parameters at $T = 500$ K

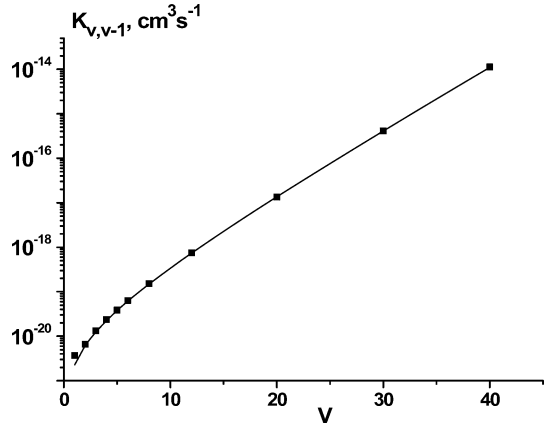

Figure 1. V−T relaxation rate coefficient for the processes $N_2(v) + N_2(v'=0) \rightarrow N_2(v-1) + N_2(v'=0)$ as a function of the vibrational quantum v at gas temperature 500 K. Filled squares show the ab initio results, the solid line shows the results obtained using the SSH-based analytical approximation.

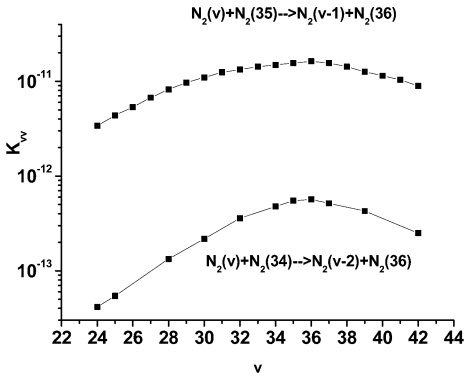

Figure 2. Single- and double-quantum V−V exchange rate coefficients for the two processes $N_2(v) + N_2(v=34) \rightarrow N_2(v-2) + N_2(v=36)$ and $N_2(v) + N_2(v=35) \rightarrow N_2(v-1) + N_2(v=36)$ as a function of vibrational quantum number $v = 500$.

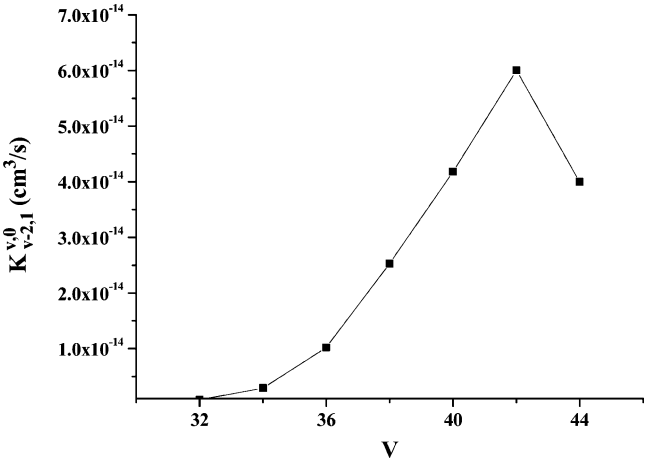

Figure 3. Asymmetric V−V exchange rate coefficients as a function of high vibrational quantum number v in the process $N_2(v) + N_2(v'=0) \rightarrow N_2(v-2) + N_2(v'=1)$.

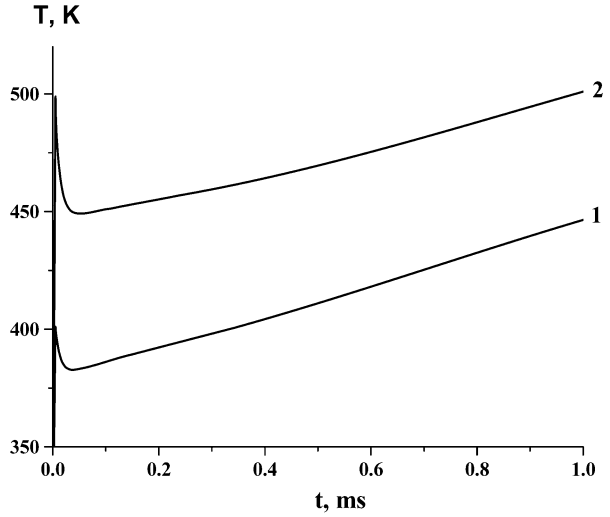

Figure 4. Gas temperature dynamics calculated for $T_F = 400$ K (line 1) and $T_F = 500$ K (line 2).

were found to be $\delta_{VT} = 0.293$ and $P_{1,0} = 0.229 \times 10^{-19}$ cm^3 s^{-1}. The only point at which the difference between the analytical approximation (eq 2.3) and the semiclassical value is not small is $K_{1,0}$ (2.29×10^{-20} cm^3 s^{-1} calculated by expression 2.3 versus 3.71×10^{-20} cm^3 s^{-1}, the numerically found value).

Figure 2 shows the behavior of the near-resonance V−V rate coefficients for the processes $N_2(v) + N_2(v'=35) \rightarrow N_2(v-1) + N_2(v'=36)$ and $N_2(v) + N_2(v'=34) \rightarrow N_2(v-2) + N_2(v'=36)$ as a function of v at $T = 500$ K. It is seen that the double-quantum exchange rate varies similarly to the single-quantum exchange rate constant while remaining essentially lower. This is a specific feature of nitrogen, that the multiquantum effects have little impact on the vibrational energy exchanges, even at such high vibrational levels.

Figure 3 presents the calculated asymmetric V−V exchange rate constants for the process $N_2(v) + N_2(v'=0) \rightarrow N_2(v-2) + N_2(v'=1)$ at the gas temperature $T = 500$ K.

It is noteworthy that the rate constant for the asymmetric near-resonant transition <0,1|42,40> is greater than that for the single-quantum resonant exchange <0,1|1,0>. Taking into account that the populations of the lowest vibrational levels are a few orders higher than that of the higher levels, a rather large influence of the near-resonant asymmetric process on the tail of the VDF at high v values is expected.

2b. Kinetic Modeling. The model includes the kinetic equations for the vibrational populations up to the vibrational level $v = 50$, which were solved self-consistently with the steady-state Boltzmann equation for the spherically symmetric part of the electron energy distribution function (EEDF) in the two-term approximation. Schematically, this last EEDF equation has the form

$$\frac{dJ_F(u)}{du} + \frac{dJ_{el}(u)}{du} = St(f_0) \qquad (2.5)$$

where u is the electron energy; J_F and J_{el} are the electron fluxes in the energy space due to the presence of the electrical field and the energy loss due to the elastic electron−molecule collisions and the rotational excitation in electron−molecule collisions, respectively; and $St(f_0)$ is the inelastic collision integral, which includes the excitation of the vibrational and electronic levels and transitions between vibrationally excited levels in electron−molecule collisions.

Reference to the collisional data concerning the electron scattering cross-sections assumed in the calculations and details on the numerical solution of the electron Boltzmann equation can be found in ref 22. In particular, when modeling the long-pulse discharge, the cross-sections for the electron-induced transitions $N_2(X^1\Sigma_g^+, v = 0) + e \rightarrow N_2(X^1\Sigma_g^+, v \leq 8) + e$ were taken from ref 23, while, for transitions between the eight lower

BATCH: jp7c14 USER: eap29 DIV: @xyv04/data1/CLS_pj/GRP_jx/JOB_i30/DIV_jp071657a DATE: July 9, 2007

vibrational levels ($1 \le v \le 8$), the cross-sections were calculated using the analytical expressions reported in ref 24.

The master equation of the vibrational kinetics can be written schematically:

$$\frac{dn_v}{dt} = R^v_{e-V} + R^v_{VV} + R^v_{VT} \quad (2.6)$$

Here R^v_{e-V}, R^v_{VV}, and R^v_{VT} are the rates of change in the population of the vth level of N_2. In particular, R^v_{e-V} is the population change due to the excitation/de-excitation processes in collisions with the plasma electrons:

$$e + N_2(v_1) \leftrightarrow e + N_2(v_2) \quad (2.7)$$

R^v_{VV} is the term due to the V−V exchange processes:

$$N_2(v) + N_2(v') \rightarrow N_2(v-\Delta v) + N_2(v'+\Delta v)$$
$$N_2(v) + N_2(v'=0) \rightarrow N_2(v-2) + N_2(v'=1) \quad (2.8)$$

Finally, R^v_{VT} is the term due the V−T vibrational relaxation processes:

$$\text{(a) } N_2(v) + N_2(v'=0) \rightarrow N_2(v-\Delta v) + N_2(v'=0) \quad (2.9)$$

$$\text{(b) } N_2(v) + N \rightarrow N_2(v-\Delta v) + N \quad (2.10)$$

As mentioned in the introduction, the complete set of the V−V and V−T/R rate constants include the data calculated in ref 8 and the additional data calculated here by the same method as that described in ref 8.

The change in the gas density after discharge initiation was calculated from an interpolating expression:

$$N(t) = N_0 \exp\left(-\frac{t}{\tau}\right) + N_0 \frac{T_0}{T}\left[1 - \exp\left(-\frac{t}{\tau}\right)\right] \quad (2.11)$$

where $\tau = \Delta r/v_s$ is the acoustic transit time; $\Delta r = 0.4$ cm is the radius of the excited region, v_s is the acoustic wave speed, and T is the current gas temperature.[12] Expression 2.11 approximately describes the transition from the isochoric regime (at short times) of gas heating to the isobaric regime (for times longer than characteristic acoustic time). The gas pressure in buffer volume was kept constant according to the experiment[12,13] and equal to 150 Torr.

The gas temperature, T, of the nitrogen gas was calculated from the thermal energy balance, taking into account the gas-dynamic expansion in the simplified manner described in ref 12.

The gas temperature was evaluated from an approximate expression:

$$\frac{dT}{dt} = \frac{W}{N \cdot C_v} + \frac{kT}{N \cdot C_v} \cdot \frac{dN}{dt} \quad (2.12)$$

where N is the gas density, C_v is the heat capacity at constant volume, and k is the Boltzmann constant. W is the overall gas heating rate associated with processes of different kinds:

$$W = W_{direct} + W_{fast} + W_{VV} + W^{asym}_{VV} + W_{VT} \quad (2.13)$$

Here, W_{direct} is the direct heating power in the discharge due to both the elastic electron−molecule collisions and the excitation of the molecular rotations by electrons; W_{fast} is the heating power caused by the fast relaxation of the electronically excited states; W_{VV}, W^{asym}_{VV}, and W_{VT} are the terms reflecting the single-quantum and asymmetric V−V exchanges and the V−T relaxation.

These terms can be expressed in the form

$$W_{VV} = \sum_{v\ge0}\sum_{i\ge1} Q^{v+1,v}_{i-1,i} n_{i-1} n_{v+1} \delta_{v+1,i} + \sum_{v\ge1}\sum_{i\ge1} Q^{i,i-1}_{v-1,v} n_i n_{v-1} \delta_{i,v} - \sum_{v\ge0}\sum_{i\ge1} Q^{i,i-1}_{v,v+1} n_i n_v \delta_{i,v+1} - \sum_{v\ge1}\sum_{i\ge1} Q^{v,v-1}_{i-1,i} n_{i-1} n_v \delta_{v,i} \quad (2.14)$$

where $Q^{v+1,v}_{i-1,i}$ is the rate constant for the V−V process $N_2(v+1) + N_2(i-1) \rightarrow N_2(v+1) + N_2(i)$; $\delta_{v+1,i} = E(v+1) - E(v) - E(i) + E(i-1)$ is the corresponding energy released in this process, and $E(v)$ is the energy of vth vibrational state.

$$W^{asym}_{VV} = \sum_{v\ge30} \{Q^{1,0}_{v-2,v} n_{v-2} n_1 \delta_{1,v} + Q^{v+2,v}_{0,1} n_{v+2} n_0 \delta_{v+2,1} - n_v (Q^{1,0}_{v,v+2} n_1 \delta_{1,v+2} + Q^{v,v-2}_{0,1} n_0 \delta_{v,1})\} \quad (2.15)$$

Here, $Q^{1,0}_{v-2,v}$ and $Q^{v+2,v}_{0,1}$ are the rate constants for the processes $N_2(v-2) + N_2(1) \rightarrow N_2(v) + N_2(0)$ and $N_2(v+2) + N_2(0) \rightarrow N_2(v) + N_2(1)$; $\delta_{1,v} = E(1) - E(0) - E(v) + E(v-2)$ and $\delta_{v+2,1} = E(v+2) - E(v) - E(1) + E(0)$ are the corresponding energy releases.

$$W_{VT} = \sum_{v\ge1} \left(Q_{v,v-1} n_v - Q_{v,v-1} \times \exp\left(-\frac{\delta_{v,v-1}}{kT}\right) n_{v-1} \right) N_{mol} \delta_{v,v-1} \quad (2.16)$$

where N_{mol} is the number of N_2 molecules per unit volume, $Q_{v,v-1}$ is the rate constant of the single quantum V−T relaxation processes $N_2(v) + N_2 \rightarrow N_2(v-1) + N_2$, and $\delta_{v,v-1}$ is the dissipated vibrational quantum energy $E(v) - E(v-1)$.

3. Results and Comparison with the Experiments

3a. Dynamics of the VDF in Pulse Discharge Afterglow. To begin, let us recall some details from the experimental measurements carried out in refs 12 and 13 of the VDF in the pulse discharge afterglow in nitrogen at a pressure of 150 Torr and an initial temperature of $T_0 = 300$ K. In ref 12, the detection of the spontaneous Raman scattering (SRS) emission was employed as the measurement technique. The SRS spectrum was excited by the 10-ns pulses of the second harmonic of a YAG:Nd^{3+} laser operating with a repetition frequency of 12.5 Hz. Generally, the scattered signal is very weak. To detect it against a background of afterglow emission, the scheme of the synchronous detection of the Stockes spectrum was employed, which measures each pulse within a 100-ns interval and accumulates the signal from 2500 pulses. The post-discharge emission of the long-lived first positive system of N_2 overlaps the spectral range of the Stockes signal. Therefore, about 1−2% of O_2 was added to quickly quench N_2 emission. Simple estimations indicate that, in these conditions, the V−T relaxation by oxygen atoms produced in the discharge can be neglected.

The nitrogen plasma, uniformly distributed in a volume of 0.5 cm^3 between the electrodes separated by a 1-cm gap, was produced by the pulsed electric discharge with a duration of 100 ns.

The vibrational kinetics was simulated taking as an initial condition the VDF measured in refs 12 and 13 for a delay time

BATCH: jp7c14 USER: eap29 DIV: @xyv04/data1/CLS_pj/GRP_jx/JOB_i30/DIV_jp071657a DATE: July 9, 2007

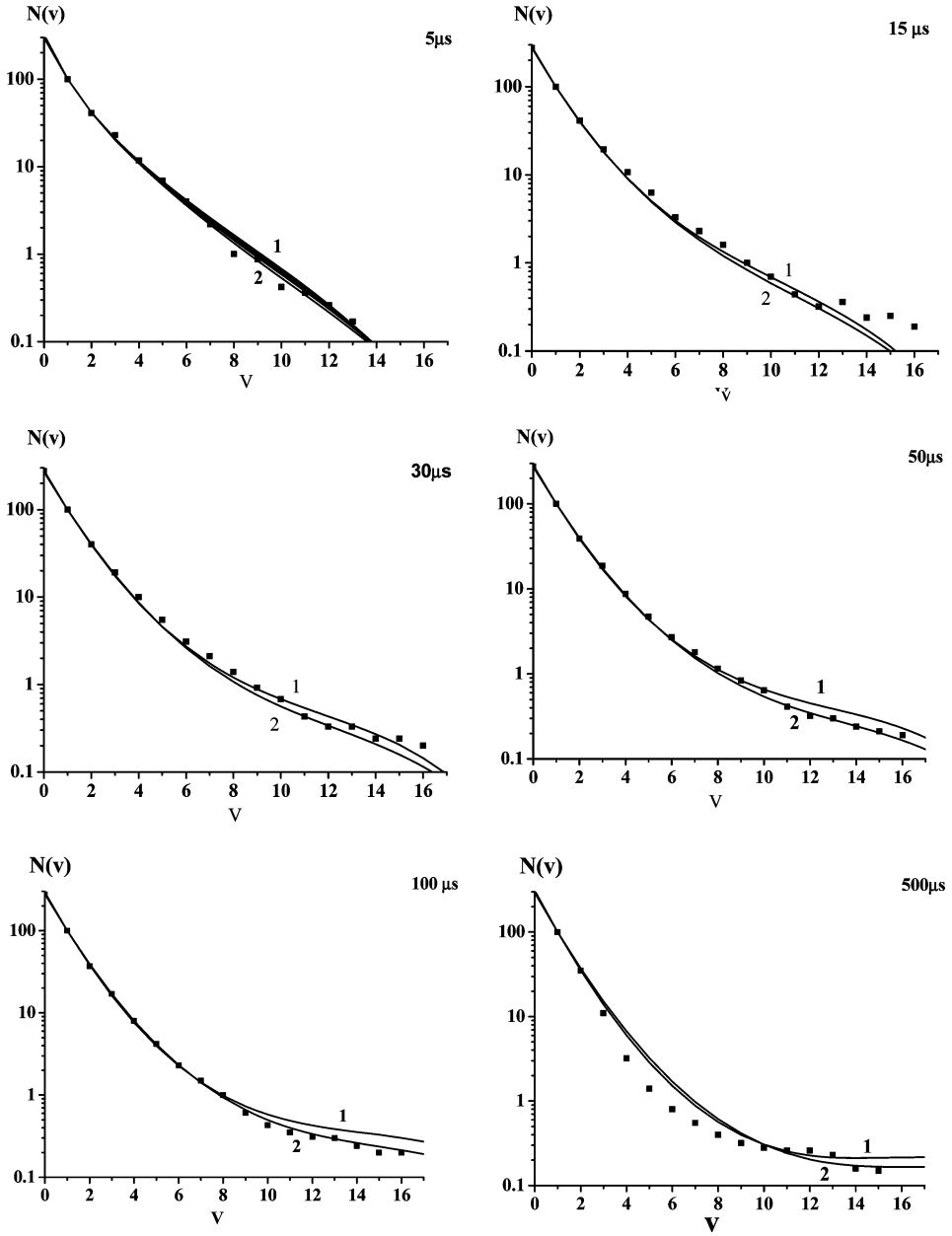

Figure 5. VDFs of the N_2 molecules calculated for $T_F = 400$ K (line 1) and $T_F = 500$ K (line 2). The distribution functions are reported at different delay times: 5, 15, 30, 50, 100, and 500 μs. The experimental data of refs 12 and 13 are shown by filled squares.

of 0.5 μs relative to the discharge pulse. The specific energy transferred into the molecular vibrations measured experimentally to this moment was 0.183 J/cm^3 (0.79 average vibration quanta per molecule).

In the mathematical treatment of the experimental data,[12,13] some uncertainty exists in the determination of the gas temperature at $t = 0.5$ μs. In fact, various collisional processes associated with the relaxation of the electronic states excited in the discharge[25] may be responsible for the observed thermal heating of the discharges, but actually these processes are not clearly identified. For this reason, the modeling of the vibrational kinetics of the N_2 molecules was carried out assuming two different rises in gas temperature values: $\Delta T = 100$ and 200 K. The calculations show that the two ΔT values have only a negligible effect on the modeling data for a heating time from 1.5 to 10 μs.

The gas-dynamic expansion of the heated gas into a large buffer volume was also taken into account.

The gas temperature evolution calculated with the procedure described above is presented in Figure 4 for two values of the initial gas temperature T_F.

The VDFs of N_2 calculated for different values of T_F are shown in Figure 5 together with the experimental vibrational populations.[12,13] In all cases, the distribution function was scaled by taking the population of the first vibrational level to equal 100. It is clearly seen that, starting from the delay time of 5 μs, the V−V exchange processes play an essential role in redistributing the vibrational populations. And indeed, the behavior of the VDF is exactly within the period (5−100 μs) that is most sensitive to the V−V exchange rate constants.

A reasonably good agreement with the experimental results is observed for delay times of 15, 30, 50, and 100 μs. At a delay time of 15 μs, the measured vibrational populations for levels $v > 12$ are abnormally large, an effect that might be explained by collisional mechanisms associated with the relaxation of the electronically excited species. In fact, in a short

BATCH: jp7c14 USER: eap29 DIV: @xyv04/data1/CLS_pj/GRP_jx/JOB_i30/DIV_jp071657a DATE: July 9, 2007

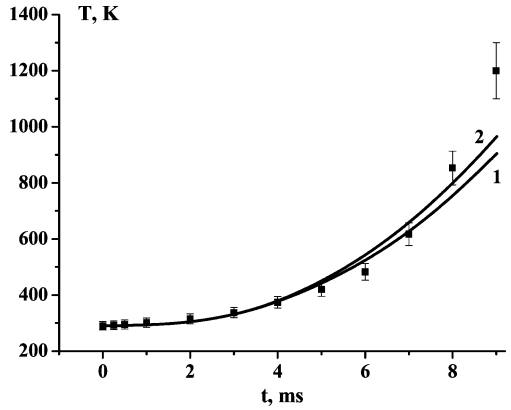

Figure 6. Time evolution of the gas temperature calculated with (curve 2) and without (curve 1) the V−T relaxation rates for the $N-N_2(v)$ collisions; filled squares are related to the experimental data.[15]

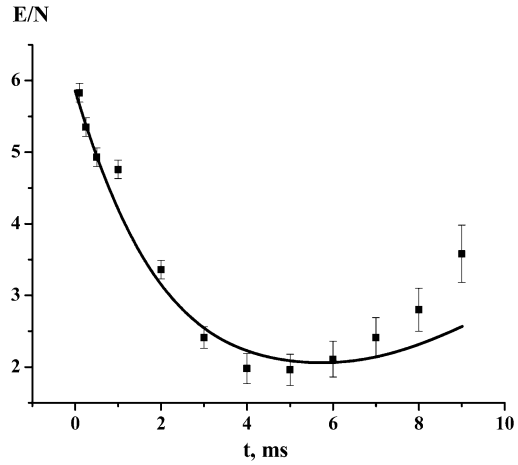

Figure 7. Comparison between the calculated (solid line) and the experimentally measured[15] (filled squares) time dependence of the reduced electric field *E*/*N*.

powerful discharge, a sizable part of the electric discharge energy causes the excitation of the electronically excited molecules which, in turn, relax with a partial energy release into the molecular vibrations.

For delay times longer than 100 μs, the changes experienced by the VDF cannot be associated with the V−V exchanges. In the region of the low-lying vibrational levels ($4 < v < 9$), the VDF measured at a delay time of 500 μs is remarkably lower than that predicted theoretically. Our estimations indicate that, on this time scale, the turbulence induced by the gas-dynamic expansion of the gas can mix gas from the inner and outer parts of the discharge, and this could explain the observed decrease in the populations of the lower vibrational levels.

3b. Time Evolution of the Gas Temperature in the Glow Discharge Regime. The kinetic model was also employed to model the process of nitrogen heating in the gas glow discharge studied experimentally.[15] Under glow discharge conditions, the vibrational motion of the nitrogen molecules is excited very effectively, which is also due to the anomalously slow V−T relaxation rates in the undissociated N_2 plasma. As a consequence, only a small part of the electric power goes to the thermal motion.

Generally, the main obstacle preventing high-energy loading in molecular vibrations is discharge constriction. Special measures were undertaken in ref 15 to sustain the uniform glow discharge in pure nitrogen with a 2-cm discharge gap length and a 3.5-cm diameter at a pressure of 50 Torr: the cathode and anode both were sectioned with ballasting by individual resistors for each section. This allows the glow discharge to operate stably up to 9 ms with a total energy input >2.5 J/L_{st}, where L_{st} is a liter at standard conditions.

Taking into account the electron energy branching fraction spent for the molecular vibrations, more than two average vibrational quanta per molecule were deposited.

For the assumed long-pulse discharge, the acoustic disturbances can be neglected, so that the discharge operation regime can be considered isobaric due to the large buffer volume. For these conditions, the gas temperature can be determined from the measured gas density using the relation $p = NkT$ (p is gas pressure, N is gas density).

The spatial distribution of the gas density was measured[15] using the interferometric method, which provides information about the discharge uniformity as well. The measurements show that the discharge uniformity is maintained throughout the pulse so that, in such conditions, the dynamics of gas heating can be reasonably well described by a zero-dimensional model.

An attempt at modeling the experimental data was undertaken in ref 15 within the framework of a self-consistent description of the plasma dynamics, but was not very successful.

Later on,[26] the self-consistent discharge model was reformulated to explain the observed evolution of the electric field and current by introducing into the model the energy-transfer processes associated with the excitation of the low-lying electronic excited states of N_2. However, no attention was paid in ref 26 to compare the gas temperature dynamics with the experiment,[15] which is, in fact, the other objective of the present investigation.

Here we used the latest and most reliable data on V−V exchange and V−T relaxation rates to simulate the experiment numerically. Both the electric field strength and the discharge current density were taken from the experiment. The initial discharge parameters used in the modeling were as follows: (i) gas temperature $T_0 = 290$ K, (ii) pressure 50 Torr, (iii) electric field strength $E_0 = 972$ V/cm, and (iv) discharge current $I_0 = 0.24$ A.

The calculated specific energy loaded into the nitrogen gas for a discharge duration of 9 ms is 2500 J/L_{st}. It should be noted that the discharge area was not determined exactly in the experiments.[15] Estimations from a visible inspection of the discharge gave a value for the discharge cross-section area in the range $S = 8-10$ cm^2. Therefore, calculations were performed assuming the two extreme values of S. It turned out that results of the simulations with $S = 8$ cm^2 are in better agreement with the experimental observation.

Figure 6 represents the calculated time evolution of the gas temperature compared with the measured variations. The theoretical results look quite satisfactory for all times except at the latest time $t = 9$ ms.

In Figure 7, the time evolution of the reduced electric field strength determined experimentally is reported and compared with the calculated *E*/*N*. Calculation was made by dividing the experimental values of E by the calculated gas density. The electric field was found in the experiments by dividing the voltage drop on plasma by the discharge spacing. The plasma voltage drop is found by subtraction of the cathode fall from the discharge voltage.

The fast reduction in the *E*/*N* parameter (see Figure 7) is explained by a specific mechanism of ionization proposed in ref 26, that is, the V−E energy exchange processes

BATCH: jp7c14 USER: eap29 DIV: @xyv04/data1/CLS_pj/GRP_jx/JOB_i30/DIV_jp071657a DATE: July 9, 2007

$$N_2(v) + N_2(v') \rightarrow N_2(a'\,^1\Sigma_u^-) + N_2 \qquad (3.1)$$

448 followed by associative ionization reactions:

$$N_2(a'\,^1\Sigma_u^-) + N_2(A\,^3\Sigma_u^+) \rightarrow N_4^+ + e \qquad (3.2)$$

$$N_2(a'\,^1\Sigma_u^-) + N_2(a'\,^1\Sigma_u^-) \rightarrow N_4^+ + e$$

449 This mechanism was not included in the present model.
450 Instead, the experimentally measured data on the discharge
451 voltage and current were exploited to extract the electric field,
452 and the discharge power density was presumed to be uniformly
453 distributed over the discharge volume. Let us emphasize that
454 this V−E exchange (eq 3.1) is quite slow in comparison with
455 the V−V exchange, hence it can be neglected in our model.
456 An important feature clearly seen in Figure 6 is the highly
457 nonlinear growth of the gas temperature with time; that is, the
458 gas-heating rate is very low initially (up to 3 ms) and then gets
459 faster and faster. It is worth considering that the glow discharge
460 is operated continuously from $t = 0$ to $t = 9$ ms. To give better
461 insight into the physical−chemical mechanisms underlying this
462 behavior of the gas temperature, Figure 8 reports the time
463 dependence of discharge power (line 1) and of the heating rates
464 for different collision processes: single-quantum V−V and
465 V−T/R exchange processes (lines 2 and 3, respectively). Figure
466 9 shows the fast discharge heating due to the elastic electron
467 collisions, excitation of the molecular rotations, and quick
468 relaxation of the electronically excited states (line 1) together
469 with the contribution due to asymmetric V−V exchanges (line
470 2), the latter making a very small contribution to gas heating.
471 From the results reported in Figure 8, it is clear that the
472 heating due to the single-quantum V−V and V−T processes is
473 dominant and, at the end of the observed time interval,
474 asymptotically reaches values close to the overall electric
475 discharge power (see Figure 8). On the other hand, the role of
476 asymmetric exchange processes is negligible, as illustrated in
477 Figure 9.
478 The direct discharge heating is rather low within the time
479 interval considered here, but it is the dominant process in the
480 earliest stages of the discharge.
481 Early on, the V−V exchange processes unexpectedly lead to
482 gas cooling instead of gas heating. This is explained by the fact
483 that, in contrast to plasma discharge in which the vibrational
484 levels above $v > 1$ are overpopulated due to the e-molecule
485 collisions, under the post-discharge conditions, the V−V
486 exchange processes are responsible for the establishment of the
487 Boltzmann-like distribution within the group of lower vibrational
488 levels. The population of the level $v = 1$ then grows at the
489 expense of the populations on the higher vibrational levels via
490 the processes $N_2(v) + N_2(0) \rightarrow N_2(v-1) + N_2(1)$. These
491 processes are endothermic and absorb energy from the thermal
492 reservoir.
493 For times greater than 1.5 ms, gas heating is controlled by
494 the energy defect released in V−V exchange processes. The
495 V−T relaxation processes come into play later and become
496 comparable with the V−V exchange input at about $t = 5$ ms.
497 However, the rate of V−T relaxation continues to grow, while
498 V−V exchange becomes less effective for the gas heating. As
499 a result, gas heating in the discharge after about 6 ms is
500 controlled by V−T relaxation processes.
501 To understand the interplay between the different mechanisms
502 relevant to the gas heating process, it is instructive to look at
503 the calculated time evolution of the VDF shown in Figure 10.

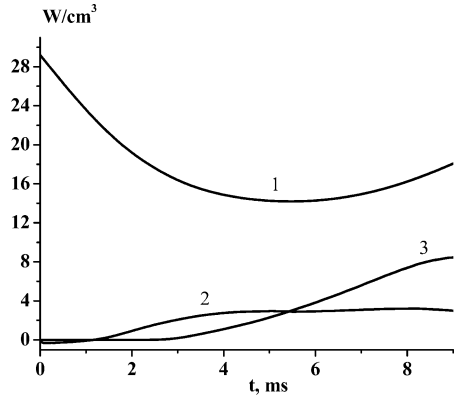

Figure 8. Time dependence of the discharge power density (line 1), reduced heating rate due to the V−V exchange processes (line 2), and the V−T relaxation (line 3). All dependences are normalized to the initial gas density.

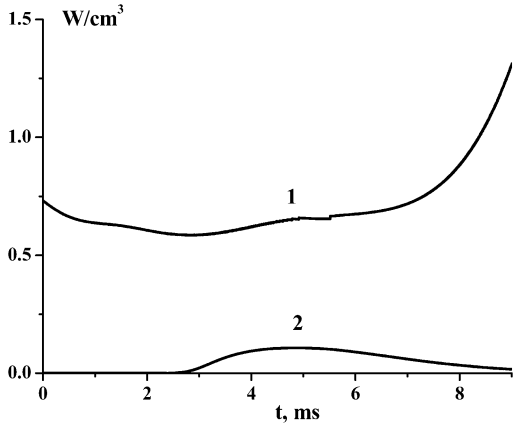

Figure 9. Time dependence of the direct discharge heating (line 1) and specific heating rate (line 2) due to the asymmetric V−V processes. All dependences are normalized to the initial gas density.

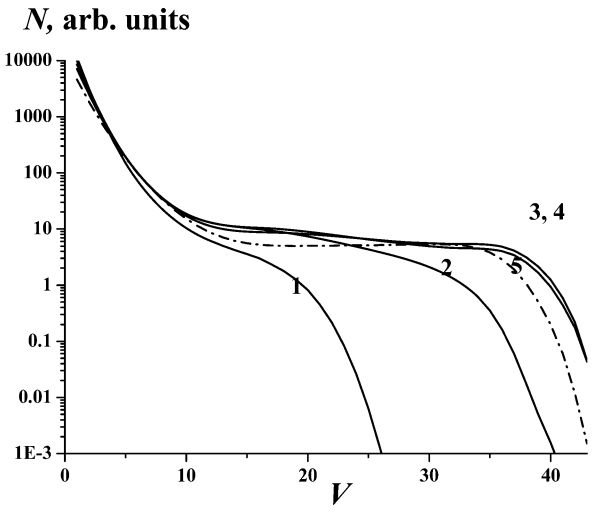

Figure 10. VDFs of $N_2(v)$ as a function of the vibrational quantum number v at different delay times: Line 1: $t = 1.5$ ms; line 2: $t = 2.5$ ms; line 3: $t = 3.5$ ms; line 4: $t = 4.5$ ms; line 5 (dash-dot line): $t = 6.5$ ms.

It is seen that, from $t = 1.5$ to $t = 3.5$ ms, the V−V exchange 504
processes lead to the population of the higher vibrational levels. 505
This period of extension of the plateau region is accompanied 506
by a rise in the heating rate associated with V−V exchanges 507
$N_2(v) + N_2(v') \rightarrow N_2(v-1) + N_2(v'+1)$, where $v < v'$. 508
Stabilization of the plateau (from 3.5 to 4.5 ms) is followed by 509
stabilization of the V−V exchange heating rate. 510

BATCH: jp7c14 USER: eap29 DIV: @xyv04/data1/CLS_pj/GRP_jx/JOB_i30/DIV_jp071657a DATE: July 9, 2007

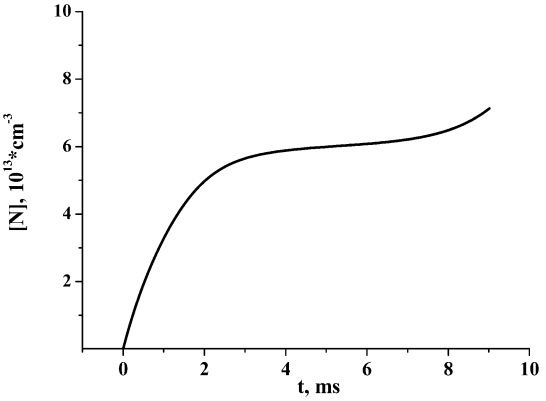

Figure 11. Time evolution of the calculated N atom concentration.

The rate constants for the V−T/R relaxation processes grow both with the vibrational level of N_2 and the gas temperature. Therefore, although the depopulation of the highest vibrational levels occurs at times longer than 6 ms, the gas-heating rate continues to grow due to the increasing of the rate constants with temperature. However, after about 8 ms, the depopulation rate of the higher vibrational levels prevails, and this would thus presumably result in a fast drop in the heating rate. However, this effect is not observed: the experimental evolution of the gas temperature in the interval between 8 and 9 ms does not confirm this prediction. The observed discrepancy could be considered an indication of a V−T relaxation rate that is faster than that assumed in the theoretical modeling. A new additional V−T relaxation mechanism appearing at this stage of the glow discharge could be associated with the accumulation of nitrogen atoms.

To test this mechanism, our model was extended so as to include the single and multiquantum V−T relaxation processes in $N-N_2$ collisions. The concentration of atomic nitrogen was calculated by adding into the system of kinetic equations the equation describing N concentration evolution in time. It was assumed that N atoms are produced in electron collisions with nitrogen molecules; recombination of atoms is too slow to exert any influence on kinetics. The N_2 dissociation rate in e-N_2 collisions was calculated by solving the Boltzmann equation for the electrons, including the dissociation cross-sections taken from ref 27. The V−T relaxation rates for single and multiquantum transitions in $N-N_2$ collisions were taken as recommended in ref 1 (eqs 7.13 and 7.14) using the analytical fit to the rate constants calculated by Laganà et al. at $T = 500$ K and $T = 1000$K reported in refs 28 and 29, respectively.

The calculated time evolution of the N atom concentration is shown in Figure 11. At the end of the pulse, the predicted atom concentration approaches a value of 7×10^{13} cm^{-3}. The time evolution of the gas temperature calculated by this extended model is represented in Figure 6 by curve 2. As can be seen, the theoretical curve does come closer to the experimental data after 8 ms, but only slightly. It is noteworthy that, although the concentration of N atoms is building up at about 3 ms, the corresponding relaxation has a more pronounced effect at the end of the pulse. Partially, this is due to the increase in the relaxation rate with the temperature and the vibrational quantum number due to the energy barrier for this process, which stems from the chemical nature of the interaction between the collision partners.

It is noteworthy that the nitrogen dissociation rate in the glow discharge is, as shown experimentally,[30] notably higher than predicted, assuming as the dissociation channel the collisions between molecular nitrogen and the electrons. In addition to that, other dissociative collisional channels, which could dominate in glow discharge, can be very effective as, for example, the collisions between vibrationally and electronically excited N_2 molecules. For this reason, the real concentration of N atoms in the experiment[15] might be higher than that predicted in Figure 11, and the growth of N atom concentration may continue up to the end of the pulse.

Thus, the role of V−T/R relaxation due to N atoms may be important for the experimental conditions explored in ref 15. The accuracy of simple analytical approximations for the single- and multiquantum V−T relaxation rates involving N atoms is questionable, so that further ab initio studies for the $N-N_2$ system are desirable, particularly for the range of higher vibrational levels and higher temperatures.

Conclusions

The complete set of the recently calculated state-to-state rate coefficients[8] provides an opportunity to simulate the vibrational kinetics in nitrogen without arbitrary and poorly grounded analytical approximations. In particular, the double-quantum and asymmetric one-to-two V−V exchange processes can be integrated into the kinetic modeling, thus removing any uncertainties associated with the use of semiempirical rates.

In this work, the detailed experimental information on the vibrational kinetics in N_2 under strong nonequilibrium conditions reported in refs 12, 13, and 15 were revisited and modeled using a modified kinetic modeling and the latest and most reliable set of the rate coefficients for V−T and V−V energy exchanges in N_2-N_2 collisions. The comparison between the simulated vibrational population dynamics and the experimental results[12,13] demonstrates that the newly calculated ab initio rate coefficients substantially improve the kinetic modeling. Usage of the same model of vibrational kinetics for numerical simulations of the measured[15] time evolution of gas temperature in the long-pulse glow discharge at a nitrogen pressure of 50 Torr allows us to describe it quite satisfactorily, except for the moment of discharge termination. It is supposed that the discrepancy between theory and experiment at the end of discharge can be explained by the relaxation of excited nitrogen molecules in collisions with N atoms. For an adequate description of the latter process, further studies are needed on the theory of N_2 and N collisions.

References and Notes

(1) Capitelli, M.; Ferreira, C. M.; Gordiets, B. F.; Osipov, A. I. *Plasma Kinetics in Atmospheric Gases*; Springer-Verlag: New York, 2000; pp 104−117.

(2) Cacciatore, M. Vibrational energy exchanges between diatomic molecules of relevance to atmospheric chemistry. In *Molecular Physics and Hypersonic Flows*; Capitelli, M., Ed.; Kluwer Academic Publishers: Norwell, MA, 1996; p 21.

(3) Millikan, R. C.; White, D. R. *J. Chem. Phys.* **1963**, *39*, 98, 3209.

(4) Henderson, M. C. *J. Acoust. Soc. Am.* **1962**, *34*, 349.

(5) Chatelet, M.; Chesnoy, J. *Chem. Phys. Lett.* **1985**, *122*, 550.

(6) Kovacs, M. A.; Mack, M. E. *Appl. Phys. Lett.* **1972**, *20*, 487.

(7) Frey, R.; Lukasik, J.; Ducuing, J. *Chem. Phys. Lett.* **1972**, *14*, 514.

(8) Cacciatore, M.; Kurnosov, A.; Napartovich, A. *J. Chem. Phys.* **2005**, *123*, 174315.

(9) Billing, G. D.; Fisher, E. R. *Chem. Phys.* **1979**, *43*, 395.

(10) Billing, G. D. *Chem. Phys. Lett.* **1980**, *76*, 178.

(11) Ahn, T.; Adamovich, I. W.; Lempert, W. R. *Chem. Phys.* **2004**, *298*, 233.

(12) Akishev, Yu. S.; Demianov, A. V.; Kochetov, I. V. *High Temp.* **1982**, *20*, 658.

(13) Podobedov, V. B. Doctor of Science Dissertation, Institute of Spectroscopy, Russian Academy of Sciences, Troitsk, Russia, 1990.

BATCH: jp7c14 USER: eap29 DIV: @xyv04/data1/CLS_pj/GRP_jx/JOB_i30/DIV_jp071657a DATE: July 9, 2007

(14) Valiansky, S. I.; Vereshchagin, K. A.; Volkov, A. Yu.; Pashinin, P. P.; Smirnov, V. V.; Fabelinsky, V. I.; Holtz, L. *Sov. J. Quantum Electron.* **1984**, *11*, 1229.

(15) Akishev, Yu. S.; Baiadze, K. V.; Vetsko, V. M.; Napartovich, A. P.; Pashkin, S. V.; Ponomarenko, V. V.; Starostin, A. N.; Trushkin, N. I. *Sov. J. Plasma Phys.* **1985**, *11*, 582.

(16) Coletti, C.; Billing, G. D. *Chem. Phys. Lett.* **2002**, *356*, 14.

(17) Billing, G.; Coletti, C.; Kurnosov, A. K.; Napartovich, A. P. *J. Phys. B* **2003**, *36*, 1175.

(18) Kurnosov, A.; Cacciatore, M.; Billing, G. D. *J. Phys. Chem. A* **2003**, *107*, 2403.

(19) Ling, M. S. H.; Rigby, M. *Mol. Phys.* **1984**, *51*, 855.

(20) Smith, N. S.; Hassan, H. A. *AIAA J.* **1976**, *14*, 374.

(21) *Non-equilibrium Air Plasmas at Atmospheric Pressure*; Becker, K. H., Kogelschatz, U., Schoenbach, K. H., Barker, R. J., Eds.; IOP Publishing: Bristol, U.K., 2004; p 216.

(22) Kochetov, I. V.; Kurnosov, A. K.; Napartovich, A. P.; Shnyrev, S. L. *Plasma Phys. Rep.* **2002**, *28*, 1041.

(23) Phelps, A. V.; Pitchford L. C. Anisotropic scattering of electrons by N_2 and its effects on electron transport: Tabulations of cross section and results. *JILA Information Center Report No. 26*; University of Colorado: Boulder, CO, 1985.

(24) Aleksandrov, N. L.; Konchakov, A. M.; Son, E. E. *Zh. Tekh. Fiz.* **1979**, *49*, 1194 (in Russian).

(25) Popov, N. A. *Plasma Phys. Rep.* **2001**, *27*, 1.

(26) Berdyshev, A. V.; Kochetov, I. V.; Napartovich, A. P. *Sov. J. Plasma Phys.* **1988**, *14*, 438.

(27) Slovetsky, D. I. Molecule dissociation by electron impact. In *Khimiya Plazmy*; Smirnov, B.M., Ed.; Atomizdat: Moscow, 1974 (in Russian).

(28) Lagana, A.; Garcia, E.; Ciccarelli, L. *J. Phys. Chem.* **1987**, *91*, 312.

(29) Armenise, I.; Capitelli, M.; Garcia, E.; Gorse, C.; Lagana, A.; Longo, S. *Chem. Phys. Lett.* **1992**, *200*, 597.

(30) Slovetsky, D. I. *The Mechanisms of Chemical Reactions in Non-equilibrium Plasmas*; Nauka: Moscow, 1980 (in Russian).